Author Manuscript

Author Manuscript

Author Manuscript

Author Manuscript

HHS Public Access

Author manuscript

Hear Res. Author manuscript; available in PMC 2015 June 14.

Published in final edited form as:

Hear Res. 2015 April ; 322: 235–241. doi:10.1016/j.heares.2015.01.004.

Temporal Resolution of ChR2 and Chronos in an Optogenetic-based Auditory Brainstem Implant Model: Implications for the Development and Application of Auditory Opsins

A. E. Hight[1,3,*], **Elliott D. Kozin**[1,2,*], **Keith Darrow**[4], **Ashton Lehmann**[1,2], **Edward Boyden**[5], **M. Christian Brown**[1,2], and **Daniel J. Lee**[1,2]

[1]Eaton-Peabody Laboratories, Massachusetts Eye and Ear Infirmary, Boston, Massachusetts

[2]Department of Otology and Laryngology, Harvard Medical School, Boston, Massachusetts

[3]Program in Speech and Hearing Bioscience and Technology, Harvard Medical School, Boston, MA

[4]Department of Communication Sciences and Disorders, Worcester State University, Worcester, Massachusetts

[5]Departments of Brain and Cognitive Sciences and Biological Engineering, MIT Media Lab and McGovern Institute, MIT, Cambridge, Massachusetts

Abstract

The contemporary auditory brainstem implant (ABI) performance is limited by reliance on electrical stimulation with its accompanying channel cross talk and current spread to non-auditory neurons. A new generation ABI based on optogenetic-technology may ameliorate limitations fundamental to electrical neurostimulation. The most widely studied opsin is channelrhodopsin-2 (ChR2); however, its relatively slow kinetic properties may prevent the encoding of auditory information at high stimulation rates. In the present study, we compare the temporal resolution of light-evoked responses of a recently developed fast opsin, Chronos, to ChR2 in a murine ABI model. Viral mediated gene transfer via a posterolateral craniotomy was used to express Chronos or ChR2 in the mouse nucleus (CN). Following a four to six week incubation period, blue light (473 nm) was delivered via an optical fiber placed directly on the surface of the infected CN, and neural activity was recorded in the contralateral inferior colliculus (IC). Both ChR2 and Chronos evoked sustained responses to all stimuli, even at high driven rates. In addition, optical stimulation evoked excitatory responses throughout the tonotopic axis of the IC. Synchrony of the light-evoked response to stimulus rates of 14–448 pulses/s was higher in Chronos compared to ChR2 mice ($p<0.05$ at 56, 168, and 224 pulses/s). Our results demonstrate that Chronos has the ability to drive the auditory system at higher stimulation rates than ChR2 and may be a more ideal opsin for manipulation of auditory pathways in future optogenetic-based neuroprostheses.

Corresponding Author: Daniel J. Lee, MD, FACS, Director, Wilson Auditory Brainstem Implant Program, Massachusetts Eye and Ear Infirmary, Associate Professor, Department of Otology and Laryngology, Harvard Medical School, 243 Charles Street, Boston, MA 02114, Daniel_Lee@meei.harvard.edu.

*Contributed equally

Author Manuscript Author Manuscript Author Manuscript Author Manuscript

Keywords

optogenetics; auditory brainstem implant; channelrhodopsin-2; Chronos; neuroprostheses; Lasker Award

1. Introduction

The cochlear implant (CI) is the most successful of neuroprosthesis, and provides meaningful auditory benefits to pediatric and adult patients with severe to profound hearing loss. In the past 50 years, over 300,000 individuals worldwide have received the CI (NIDCD, 2014), as the technology has evolved from a crude single channel implant to a multichannel auditory neurostimulator providing sound and speech perception to the majority of deaf users. The recent Lasker Award highlights the development of the CI and illustrates the profound success of this device and its positive impact on society (Williams, 2013). However, there is a small subset of deaf individuals who will not benefit from the CI due to 1) a small or absent cochlea, 2) a small or absent auditory nerve, or 3) injury or scarring of the inner ear or auditory nerve secondary to meningitis, trauma, or tumor, such as bilateral vestibular schwannomas that arise from Neurofibromatosis-2 (NF-2; (Asthagiri *et al.*, 2009). An auditory brainstem implant (ABI) is an option to provide hearing sensations in these patients who are not candidates for the CI due to anatomic considerations. More than 1,000 patients worldwide have been implanted with an ABI (Lin *et al.*, 2012). The ABI bypasses the damaged or absent cochlea and auditory nerve to transmit electrical stimuli to the cochlear nucleus (CN) in the brainstem (Hitselberger *et al.*, 1984; Sennaroglu *et al.*, 2009).

Hearing outcomes of ABI users are highly variable across similar cohorts of patients (Colletti *et al.*, 2012; Colletti and Shannon, 2005; Nevison *et al.*, 2002), and overall performance with the ABI lag behind those seen with the CI. Further, many ABI users experience side effects, such as pain, facial twitching, and dizziness, due to activation of non-auditory neurons (Colletti *et al.*, 2010). A possible explanation for the wide range of outcomes and side effects may be the spread of electric current (Eisen and Franck, 2005; Nardo *et al.*, 2008; Venter and Hanekom, 2014). One approach to improve speech perception is to increase the number of electrode channels. However, due to current spread, this may result in channel cross talk (Boe_x *et al.*, 2003; Karg *et al.*, 2013; Qazi *et al.*, 2013).

Optical stimulation of the nervous system is now being used as a novel stimulus paradigm in research laboratories. For the central auditory system, light-based activation of offers a theoretical advantage over traditional electric-based neural stimulation as focused light may be able to excite a select set of neurons, increasing the density of independent stimulation channels while reducing the unintended consequence of current spread (Fu and Nogaki, 2005; Fu *et al.*, 1998). These properties could address the limitations seen with the electrically based ABI. Over the past decade, infrared neural stimulation (INS) of the auditory system has been investigated, however, the approach may be limited by risk of thermal tissue injury, potential optophonic artifacts, and lack of response to stimulation of the CN (Hirase *et al.*, 2002; Verma *et al.*, 2014; Wells *et al.*, 2007).

Author Manuscript Author Manuscript Author Manuscript Author Manuscript

In contrast to INS, optogenetics uses visible light from the visible spectrum to stimulate the nervous system, and it has been used to investigate a host of neural systems (Ayling *et al.*, 2009; Boyden *et al.*, 2005; Huff *et al.*, 2013; Rolls *et al.*, 2011). Viral -mediated infection is a common approach to deliver light-sensitive microbial opsin genes and enable neurons to respond to optical stimulation. ChR2 is the most widely used opsin in neuroscience, (Bernstein *et al.*, 2008; Boyden *et al.*, 2005; Chow *et al.*, 2010; Han and Boyden, 2007; Zhang *et al.*, 2006), however, only a few recent studies have applied optogenetics to the auditory system.(Hernandez *et al.*, 2014; Shimano *et al.*, 2013) Shimano *et al.* introduced ChR2 into the CN and demonstrated light-evoked increases in auditory neural activity locally in the CN. Building on Shimano *et al.*, we previously showed optogenetic stimulation of the CN results in activation of the upstream auditory pathway, including the inferior colliculus and auditory cortex (Darrow *et al.*, 2013). In a more recent study by Hernandez *et al. 2014*, responses were evoked by stimulation of the peripheral auditory system in transgenic mice expressing ChR2 in spiral ganglion neurons of the cochlea. Overall, these studies demonstrate that optogenetics can be used to activate the auditory system from the periphery throughout the central pathway.

One of the unique properties of the auditory system is its capability provide a high synchrony of response, a property necessary to encode the rapidly varying characteristics of speech. Original studies of the kinetics of ChR2 and its variants suggest that ChR2 may be too slow for optimal function in the auditory system (Boyden *et al.*, 2005; Darrow *et al.*, 2013; Zhang *et al.*, 2006). Over the last several years, a host of new opsins have become available with variable activation thresholds, wavelengths of stimulation, and, most importantly, kinetic properties (Yizhar *et al.*, 2011). One of the most recently developed opsins, Chronos, appears to have faster kinetic properties that may better suited to temporal characteristics of the auditory system (Klapoetke *et al.*, 2014). Herein, we compare the temporal characteristics of ChR2 and Chronos in a translational murine ABI model.

2. Methods

2.1 Animal Protocol

All experimental procedures were performed in accordance with the National Institutes of Health guidelines for the care and use of laboratory animals as well as the approved animal care and use protocols at the Massachusetts Eye & Ear Infirmary, Boston, MA.

2.2 Surgical Exposure of the Dorsal Cochlear Nucleus

Methods to expose the dorsal cochlear nucleus (DCN) have been described recently described (Kozin *et al.*, 2014). Direct exposure of the DCN, rather than stereotaxic injection, was used to minimize the chances of missing the desired injection site as well as replicate the potential surgical approach in human ABI operation. Normal hearing CBA/CaJ mice aged 8–12 weeks are anesthetized with xylazine 20 mg/kg and ketamine 100 mg/kg via an intraperitoneal administration. Following anesthesia, the overlying the scalp is exposed to provide unobstructed access to the surgical site. The mouse is placed in a Kopf small animal stereotaxic holder (Tujunga, CA), and held in place by a snout clamp. The left parietal, interparietal, and occipital bones of the skull are exposed and rongeurs are used to make a

Author Manuscript Author Manuscript Author Manuscript Author Manuscript

craniotomy over the interparietal bone, left of midline, ~2 mm caudal to the lambda suture line. Following craniotomy, using a 5 French suction, aspiration of lateral-most portion of the left cerebellum reveals the underlying DCN. (Fig. 1).

2.3 Pressure Microinjection for Gene Transfer

After the DCN was clearly visible, pressure microinjections are made into the DCN using a 5 μl Hamilton syringe. We used between 1.5–2.0 μl of adeno-associated virus with ChR2 (AAV2.8-ChR2 fused with GFP or mCherry and CAG promoter) or Chronos (AAV2.8-ChR2 fused with GFP and CAG promoter) for 2–4 min. Immediately following injection, the incision was closed and the scalp was sutured. Four additional mice were used as either 'sham' or control cases. These included sham-injected mice (n=2) that underwent the exact surgical protocol as AAV injected mice, including insertion of an empty Hamilton syringe in to the brainstem for 2–4 minutes, and control mice (n=2), which have no history of manipulation.

2.4 Re-exposure of Dorsal Cochlear Nucleus and Exposure of Contralateral Inferior Colliculus

After a 3–6 week survival time to allow for neuron transduction and expression of the ChR2 or Chronos, the mice were prepared for acute surgery to characterize responses to optical stimulation. Mice were re-anesthetized and underwent the above-described surgical procedure. After the injected region was re-exposed for optical stimulation, a craniotomy was made over the right IC and the brain surface was covered with high-viscosity silicon oil. During the course of physiological recordings, the core body temperature of the animal was maintained at 36.8°C with a homeothermic blanket system.

2.5 Optical Stimulation

Optical stimuli were produced by a laser (BL473T-100FC, Shanghai Laser & Optics Century Co.) and an optical fiber (400 μm diameter) placed directly over the exposed surface of the DCN. (Fig. 1) Blue light (473 nm) pulses of 1 ms duration were presented at pseudorandomized rates from 14–448 pulses/s for train durations of 300 or 500 ms followed by 300 or 500 ms of no stimulation, respectively. For both protocols, either 50 or 80 trials were presented at light intensity ranging from 0 to 200 mW/mm^2. The laser was calibrated by positioning the optical fiber 2 mm from a high-sensitivity thermopile sensor (Coherent PS19Q) connected to a power meter (Coherent LabMax-TOP). The voltage command parameters were systematically varied, and the measured power was divided by the cross-sectional area of the fiber and pulse rate to get the laser intensity (radiant exposure) in mW/mm^2.

2.6 Contralateral Inferior Colliculus Recordings

Multiunit recordings were made from the central nucleus of the IC using a penetrating 16-channel linear silicone probe (NeuroNexus Technologies, Fig. 1). The position of the recording probe was optimized to generate a complete tonotopic map across the recording channels (Guo *et al.*, 2012; Malmierca *et al.*, 1993) using acoustic frequencies from 8 to 45.25 kHz in 0.5 octave steps and from 0–80 dB in 10 dB steps, using 20 ms duration tone

Author Manuscript Author Manuscript Author Manuscript Author Manuscript

bursts with a repetition rate of 10 bursts/s. Raw voltage signals were band-pass filtered (0.3–3 kHz, 5 pole) and sampled at 25 kHz (Plexon). Common mode rejection was performed across all 16 channels and then the signal was digitally filtered (zero-phase butterworth band-pass filter, 0.5–3 kHz, 5-pole). To compute average firing rate, spike count was computed over the pulse train duration. Spontaneous firing rate was computed from spikes collected during the no stimulation period. Driven rate was computed by subtracting the spontaneous rate from the firing rate during the stimulus. Paired t-tests were computed between the firing rate and spontaneous rate from every trial for an electrode and stimulus intensity. For each electrode-intensity combination in which $p>0.01$, the driven rate was assigned to be 0 spikes/second. Driven rate-intensity curves were generated from the average of driven rate across all electrodes collected during each stimulus intensity presented at 28 pulses/s. To investigate temporal properties of laser-evoked spiking we computed the synchronization index (SI, magnitude of the vector of averaged spikes collected during the period between stimulus pulses; the SI varies between 0 (no synchronization) and 1 (all spikes occurring exactly at the same phase of the stimulus period) (Dynes and Delgutte, 1992). For all stimulus electrode-intensities in which driven rate was calculated to be zero spikes/s, SI was also set to zero.

2.7 Histology and Immunohistochemistry

Following conclusion of experiments, mice were euthanized with an overdose of ketamine and perfused with normal saline followed by 4%paraformaldehyde. Brainstems were extracted from the skull and post-fixed for 2 hours. Brainstems were cryoprotected in 30% sucrose for 48 hours, and then sectioned using a cryostat using 30–60 μm sections. Before the staining procedure, sections were allowed to dry at room temperature and then rehydrated in PBS for 10 min. After washing with PBS, tissue was permeabilized and blocked with blocking solution (0.3% Triton X-100, 15% heat inactivated goat or donkey serum in PBS) for 1 hour. Visualization of nuclei was performed with 4,6-diamidino-2-phenylindole (DAPI), (Vector Laboratories). Staining was analyzed with epifluorescence microscopy (Axioskop2 Mot Axiocam, Zeiss) and confocal microscopy (TCD, Leica).

3. Results

3.1 Expression of Chronos and ChR2 in the Cochlear Nucleus

Opsin-linked fluorescence demonstrated Chronos or ChR2 transfer throughout the DCN. Labeling was observed in all three CN subdivisions including clear labeling of neurons in the fusiform cell layer of the DCN. Chronos localized to both neuronal-specific and non-neuronal populations. In the neuronal populations, there is involvement of a wide array of CN cell types, including morphologies consistent with DCN fusiform cells (red arrow, Fig. 2B), giant cells, and cartwheel-like cells.

3.2 Synchronization and Driven Rate of IC Neural Activity in Response to Optical Stimulation of CN

Clear neural activation in the IC was evoked by light stimulation of the CN. Dot raster and peristimulus time (PST) histogram plots from one electrode of a Chronos mouse is shown in Figure 3. High, sustained rates of firing are observed during the light pulse trains and low

Author Manuscript Author Manuscript Author Manuscript Author Manuscript

rates of spontaneous firing are observed when there are no stimuli (second half of traces). For the pulse train of 448 pulses/s (Fig. 3B), the PST histogram shows that the high initial firing adapted to steady-state firing over the course of the 500-ms pulse train. This adaptation was not present for the low rate (Fig. 3A), even though the overall firing rate was greater. However, for all pulse rates tested, the driven rate was sustained above spontaneous firing.

The temporal pattern of firing depends on pulse rate. For the train of pulses at 28 pulses/s (Fig. 3A), the activity is synchronized to the pulses, whereas for the train of pulses at 448 pulses/s (Fig. 3B), the activity, though high, appears to be less synchronized. The average SI values are shown for Chronos and ChR2 cases in Figure 4A. For both opsins, there is a decline in SI with increasing pulse rate. For all pulse rates, recordings from Chronos mice had higher SI than those from ChR2 mice. These differences were significant at rates of 56, 168 and 224 pulses/s (Fig. 4A, asterisks). The decline in synchrony with increasing pulse rates was not due to a decline in firing rate, since driven rate was significant at all tested stimulus rates (14–448 pulses/s, Fig. 4B). Even at high pulse rates (e.g. 448 pulses/s), driven rates were high despite the compromised kinetics of both Chronos and ChR2. Further, the firing rates of mice injected with Chronos or ChR-2 were increasing, monotonic functions of laser intensity, with evidence of incomplete saturation at the highest intensities (Fig. 5B). At these intensities, average firing rates were significantly lower for ChR2 versus Chronos ($p < 0.001$, avg. rate 126.649 spikes/s for Chronos vs. 54.73 spikes/s for ChR2 at ~100 mW/mm^2).

3.3 Spatial Pattern of Response for Optogenetic-based Stimulation of the Cochlear Nucleus

There was variability in the spatial pattern of responses from case to case. Figure 5A shows a case where nearly all electrodes recorded laser-evoked activity for stimulus levels at and above threshold (driven rate > 0 spikes/s, indicated by non-dark blue coloring). Highest spike rates were observed on electrodes 2–8. Other cases (data not shown) had variable patterns of neural activation: of the 16 electrodes, the average number activated across all laser intensities at and above threshold (stimulus rate = 28 pules/second) was 12.4 with a range of 9–14.9 electrodes for Chronos (n=4 mice) and 9.2 with a range of 4.6–14 electrodes for ChR2 (n=4 mice). Sham and control mice showed no response to optical stimulation (one example shown in Fig. 5C).

4. Discussion

4.1 Chronos versus ChR2 for Light-Evoked Activation of the Auditory System

Our study is the first to characterize the temporal properties of opsins in the auditory system. Of all presently studied opsins, Chronos, has the fastest on/off kinetics (Klapoetke *et al.*, 2014), however, these kinetics have been previously explored only in cultured neurons. For *in vivo* stimulation of the CN, we found that Chronos has better synchrony compared to ChR2. For both opsins, there was a decline in SI with increasing pulse rates however the decline was more pronounced for ChR2. Significant differences between the two opsins were found at 56, 168 and 224 pulses/s. The high end of these pulse rates are important

Author Manuscript Author Manuscript Author Manuscript Author Manuscript

because contemporary clinical ABI processors employing the SPEAK sound processing strategy use pulse rates of 250 pulses/s.

Although the temporal properties of optogenetic responses have not been characterized previously, the responses of IC neurons to electrical stimulation of the cochlea have previously been reported. Responses of IC neurons to electrical stimulation of the cochlea also decline with increasing pulse rates, and their synchrony measures are comparable to the optogenetic responses reported here (Middlebrooks and Snyder, 2010; Snyder *et al.*, 1995). In addition, synchrony is even higher in IC recordings from awake animals (Chung *et al.*, 2014). In those studies, differences among types of units were observed, with some units able to fire synchronously to high rates (> 100 pulses/s) whereas others unable to synchronize to these rates. In the present study, such differences were not documented because the multi-unit recordings used probably sample from a combination of unit types.

For optogenetic stimulation, even for pulse rates for which responses were nonsynchronized, driven rates were substantial (Fig. 3B). Further, since rate-intensity curves (Fig. 5B) suggest that the entire dynamic range of the response was not captured due to the limits of our laser, a higher-intensity stimulus would likely produce even higher driven rates. Such driven rates will signal the presence of a stimulus even though there is little synchrony to the fine time structure of the stimulus.

4.2 Limitations of Viral-mediated Gene Transfer

There are inherent limitations to viral mediated gene transfer in the central nervous system that may have influence our results. We previously demonstrated that expression of opsins as a result of viral mediated gene transfer is variable from case to case (Darrow *et al.*, 2014; Darrow *et al.*, 2013). Consequently, the locations and numbers of activated cells may differ. This may affect synchrony because, at least for responses to acoustic stimuli, different types of neurons have different temporal characteristics(Young, 1984). In particular, fusiform cells of the DCN can express Chronos (Fig. 2B) and ChR2(Darrow *et al.*, 2014; Darrow *et al.*, 2013), and these large principal cells which project directly to the IC (Oliver and Morest, 1984) may have mediated much of the excitatory responses observed here. Finally, driven spike rates, which could vary depending on the type and number of opsin-expressing neurons, could affect the calculation of SI, but we observed high driven spike rates for both opsins.

4.3 Translational Models and Future Optogenetics Research in the Central Auditory System

In addition to examining the temporal properties of Chronos and ChR2, we demonstrate a feasible translational approach for gene transfer of opsins to the CN. Specifically, our surgical approach in the murine model allows for visualization of the DCN and inoculation with a viral gene transcript. In many respects, our model is analogous to surgical approach of the human ABI placement. While viral mediated gene transfer has inherent weaknesses and risks, numerous FDA-approved gene therapy studies are ongoing and it remains an available tool for gene transfer in humans.

Author Manuscript Author Manuscript Author Manuscript Author Manuscript

Further, our study represents the beginning of a path toward the particular opsin chosen for an eventual prosthesis. We define the ideal characteristics of an “auditory opsin” for use in a neuroprosthesis: 1) fast temporal kinetics to encode speech information, 2) low activation threshold to decrease energy requirements from an external power source, and 3) a promoter that enables tissue-specific selectivity so that only or mainly CN neurons express the opsin. Indeed, looking forward, our study raises several questions: What is the ideal gene transfer approach for delivery of opsins to the auditory system? What is the long-term safety profile of opsins, and will there be any deleterious effects on remaining hearing? Finally, can optogenetic-based stimulation function as replacement to electrical stimulation, or simply as an adjunct? The answers to these questions, both in the central and peripheral auditory systems, remain to be seen and should be the focus of future studies.

5. Conclusion

Previous studies have demonstrated the feasibility of an optogenetic stimulation for light-based activation of the central auditory system. Currently, the most widely used opsin in neuroscience is ChR2, however, it may not possess the temporal properties necessary to encode auditory information. In this study, we present the first characterization of the temporal properties of opsins in the auditory system by exploring both ChR2 and a newly engineered faster opsin, Chronos. We find in an ABI model Chronos has significantly improved kinetic properties compared to ChR2. These studies highlight the need to further examine and identify the ideal “auditory opsin” that can support the high stimulation rates needed for the transfer of temporal cues along the auditory pathways. Future studies may seek to design opsins optimized for new generation ABI based on light.

Acknowledgments

Preliminary results of this study were presented at the Association for Research in Otolaryngology Midwinter Meeting, February 2013 and 2014. This work was supported by a Fondation Bertarelli grant (D.J.L and S.L), a MED-EL grant (D.J.L), and National Institutes of Health Grants DC01089 (M.C.B.), T32 DC000038 (A.E.H.), T32 DC000020 (E.D.K).

References

Asthagiri A, Parry D, Butman J, Kim H, Tsilou E, Zhuang Z, Lonser R. Neurofibomatosis type 2. Lancet. 2009; 373:1974–1986. [PubMed: 19476995]

Ayling OG, Harrison TC, Boyd JD, Goroshkov A, Murphy TH. Automated light-based mapping of motor cortex by photoactivation of channelrhodopsin-2 transgenic mice. Nat Methods. 2009; 6:219–24. [PubMed: 19219033]

Bernstein JG, Han X, Henninger MA, Ko EY, Qian X, Franzesi GT, McConnell JP, Stern P, Desimone R, Boyden ES. Prosthetic systems for therapeutic optical activation and silencing of genetically-targeted neurons. Proc Soc Photo Opt Instrum Eng. 2008; 6854:68540H.

Boëx C, de Balthasar C, Kós MI, Pelizzone M. Electrical field interactions in different cochlear implant systems. J Acoust Soc Am. 2003; 114:2049. [PubMed: 14587604]

Boyden ES, Zhang F, Bamberg E, Nagel G, Deisseroth K. Millisecond-timescale, genetically targeted optical control of neural activity. Nat Neurosci. 2005; 8:1263–1268. [PubMed: 16116447]

Chow BY, Han X, Dobry AS, Qian X, Chuong AS, Li M, Henninger MA, Belfort GM, Lin Y, Monahan PE, Boyden ES. High-performance genetically targetable optical neural silencing by light-driven proton pumps. Nature. 2010; 463:98–102. [PubMed: 20054397]

Author Manuscript Author Manuscript Author Manuscript Author Manuscript

Chung Y, Hancock KE, Nam SI, Delgutte B. Coding of electric pulse trains presented through cochlear implants in the auditory midbrain of awake rabbit: comparison with anesthetized preparations. J Neurosci. 2014; 34:218–31. [PubMed: 24381283]

Colletti L, Shannon R, Colletti V. Auditory brainstem implants for neurofibromatosis type 2. Curr Opin Otolaryngol Head Neck Surg. 2012; 20:353–7. [PubMed: 22886036]

Colletti V, Shannon RV. Open set speech perception with auditory brainstem implant? Laryngoscope. 2005; 115:1974–1978. [PubMed: 16319608]

Colletti V, Shannon R, Carner M, Veronese S, Colletti L. Complications in Auditory Brainstem Implant Surgery in Adults and Children. Otol Neurotol. 2010; 31:558–564. [PubMed: 20393378]

Darrow K, Slama C, Owoc M, Kozin E, Hancock K, Kempfle J, Edge A, Lacour A, Boyden W, Polley D, Brown M, Lee D. Optogenetic stimulation of the cochlear nucleus using channelrhodopsin-2 evokes activity in the central auditory pathway. Brain Research. 2014 Submitted.

Darrow, KN.; Slama, M.; Kempfle, J.; Boyden, E.; Polley, D.; Brown, MC.; Lee, DJ. Optogenetic control of central auditory neurons. Association for Research in Otolaryngology MidWinter Meeting; Baltimore, MD. 2013.

Dynes S, Delgutte B. Phase-locking of auditory-nerve discharges to sinusoidal electric stimulation of the cochlea. Hear Res. 1992; 58:79–90. [PubMed: 1559909]

Eisen MD, Franck KH. Electrode interaction in pediatric cochlear implant subjects. J Assoc Res Otolaryngol. 2005; 6:160–70. [PubMed: 15952052]

Fu Q, Nogaki G. Noise susceptibility of cochlear implant users: the role of spectral resolution and smearing. J Assoc Res Otolaryngol. 2005; 6:19–27. [PubMed: 15735937]

Fu QJ, Shannon RV, Wang X. Effects of noise and spectral resolution on vowel and consonant recognition: acoustic and electric hearing. J Acoust Soc Am. 1998; 104:3586–96. [PubMed: 9857517]

Guo W, Chambers A, Darrow K, Hancock K, Shinn-Cunningham B, Polley D. Robustness of cortical topography across fields, laminae, anesthetic states, and neurophysiological signal types. J Neurosci. 2012; 32:9159–72. [PubMed: 22764225]

Han X, Boyden ES. Multiple-color optical activation, silencing, and desynchronization of neural activity, with single-spike temporal resolution. PLoS ONE. 2007; 2:e299. [PubMed: 17375185]

Hernandez VH, Gehrt A, Reuter K, Jing Z, Jeschke M, Mendoza Schulz A, Hoch G, Bartels M, Vogt G, Garnham CW, Yawo H, Fukazawa Y, Augustine GJ, Bamberg E, Kugler S, Salditt T, de Hoz L, Strenzke N, Moser T. Optogenetic stimulation of the auditory pathway. J Clin Invest. 2014; 124:1114–29. [PubMed: 24509078]

Hirase H, Nikolenko V, Goldberg JH, Yuste R. Multiphoton stimulation of neurons. J Neurobiol. 2002; 51:237–47. [PubMed: 11984845]

Hitselberger W, House W, Edgerton B, Whitaker S. Cochlear nucleus implant. Otolaryngol Head Neck Surg. 1984; 92:52–4. [PubMed: 6422415]

Huff ML, Miller RL, Deisseroth K, Moorman DE, LaLumiere RT. Posttraining optogenetic manipulations of basolateral amygdala activity modulate consolidation of inhibitory avoidance memory in rats. Proc Natl Acad Sci U S A. 2013; 110:3597–602. [PubMed: 23401523]

Karg S, Lackner C, Hemmert W. Temporal interaction in electrical hearing elucidates auditory nerve dynamics in humans. Hear Res. 2013; 299:10–8. [PubMed: 23396273]

Klapoetke NC, Murata Y, Kim SS, Pulver SR, Birdsey-Benson A, Cho YK, Morimoto TK, Chuong AS, Carpenter EJ, Tian Z, Wang J, Xie Y, Yan Z, Zhang Y, Chow BY, Surek B, Melkonian M, Jayaraman V, Constantine-Paton M, Wong GK, Boyden ES. Independent optical excitation of distinct neural populations. Nat Methods. 2014; 11:338–46. [PubMed: 24509633]

Kozin E, Darrow K, Hight A, Lehmann A, Kaplan A, Brown M, Lee D. Direct Visualization of the Murine Dorsal Cochlear Nucleus for Optogenetic Stimulation of the Auditory Pathway. JoVE. 2014 In press.

Lin, H.; Herrmann, B.; Lee, D. Auditory Brainstem Implants. Plural Publishing; San Diego: 2012.

Malmierca MS, Blackstad TW, Osen KK, Karagulle T, Molowny RL. The central nucleus of the inferior colliculus in rat: A Golgi and computer reconstruction study of neuronal and laminar structure. J Comp Neurol. 1993; 333:1–27. [PubMed: 7688006]

Author Manuscript Author Manuscript Author Manuscript Author Manuscript

Middlebrooks JC, Snyder RL. Selective electrical stimulation of the auditory nerve activates a pathway specialized for high temporal acuity. J Neurosci. 2010; 30:1937–46. [PubMed: 20130202]

Nardo WD, Cantore I, Marchese MR, Cianfrone F, Scorpecci A, Giannantonio S, Paludetti G. Electric to acoustic pitch matching: a possible way to improve individual cochlear implant fitting. Eur Arch Otorhinolaryngol. 2008; 265:1321–8. [PubMed: 18379812]

Nevison B, Laszig R, Sollmann W, Lenarz T, Sterkers O, Ramsden R, Fraysse B, Manrique M, Rask-Andersen H, Garcia-Ibanez E, Colletti V, von Wallenberg E. Results from a European clinical investigation of the Nucleus multichannel auditory brainstem implant. Ear Hear. 2002; 23:170–83. [PubMed: 12072610]

NIDCD. Cochlear Implants [Online]. 2014. http://wwwnidcdnihgov/health/hearing/pages/cochaspx (verified 8/18/2014)

Oliver DL, Morest DK. The central nucleus of the inferior colliculus in the cat. J Comp Neurol. 1984; 222:237–264. [PubMed: 6699209]

Qazi O, van Dijk B, Moonen M, Wouters J. Understanding the effect of noise on electrical stimulation sequences in cochlear implants and its impact on speech intelligibility. Hear Res. 2013; 299:79–87. [PubMed: 23396271]

Rolls A, Colas D, Adamantidis A, Carter M, Lanre-Amos T, Heller HC, de Lecea L. Optogenetic disruption of sleep continuity impairs memory consolidation. Proc Natl Acad Sci U S A. 2011; 108:13305–10. [PubMed: 21788501]

Sennaroglu L, Ziyal I, Atas A, Sennaroglu G, Yucel E, Sevinc S, Ekin M, Sarac S, Atay G, Ozgen B, Ozcan O, Belgin E, Colletti V, Turan E. Preliminary results of auditory brainstem implantation in prelingually deaf children with inner ear malformations including severe stenosis of the cochlear aperture and aplasia of the cochlear nerve. Otol Neurotol. 2009; 30:708–15. [PubMed: 19704357]

Shimano T, Fyk-Kolodziej B, Mirza N, Asako M, Tomoda K, Bledsoe S, Pan ZH, Molitor S, Holt AG. Assessment of the AAV-mediated expression of channelrhodopsin-2 and halorhodopsin in brainstem neurons mediating auditory signaling. Brain Res. 2013; 1511:138–52. [PubMed: 23088961]

Snyder R, Leake P, Rebscher S, Beitel R. Temporal resolution of neurons in cat inferior colliculus to intracochlear electrical stimulation- effects of neonatal deafening and chronic stimulation. J Neurophysiol. 1995; 73:449–67. [PubMed: 7760111]

Venter P, Hanekom J. Is There a Fundamental 300 Hz Limit to Pulse Rate Discrimination in Cochlear Implants? J Assoc Res Otolaryngol. 2014 In press.

Verma RU, Guex AA, Hancock KE, Durakovic N, McKay CM, Slama MC, Brown MC, Lee DJ. Auditory responses to electric and infrared neural stimulation of the rat cochlear nucleus. Hear Res. 2014; 310:69–75. [PubMed: 24508368]

Wells JD, Thomsen S, Whitaker P, Jansen ED, Kao CC, Konrad PE, Mahadevan-Jansen A. Optically mediated nerve stimulation: Identification of injury thresholds. Lasers Surg Med. 2007; 39:513–26. [PubMed: 17659590]

Williams C. Hearing restoration: Graeme Clark, Ingeborg Hochmair, and Blake Wilson receive the 2013 Lasker~DeBakey Clinical Medical Research Award. J Clin Invest. 2013; 123:4102–6. [PubMed: 24091320]

Yizhar O, Fenno LE, Davidson TJ, Mogri M, Deisseroth K. Optogenetics in neural systems. Neuron. 2011; 71:9–34. [PubMed: 21745635]

Young, ED. Response characteristics of neurons of the cochlear nuclei. In: Berlin, CI., editor. Hearing Science: Recent Advances. College-Hill Press; San Diego: 1984. p. 423-460.

Zhang F, Wang LP, Boyden ES, Deisseroth K. Channelrhodopsin-2 and optical control of excitable cells. Nat Methods. 2006; 3:785–92. [PubMed: 16990810]

Author Manuscript Author Manuscript Author Manuscript Author Manuscript

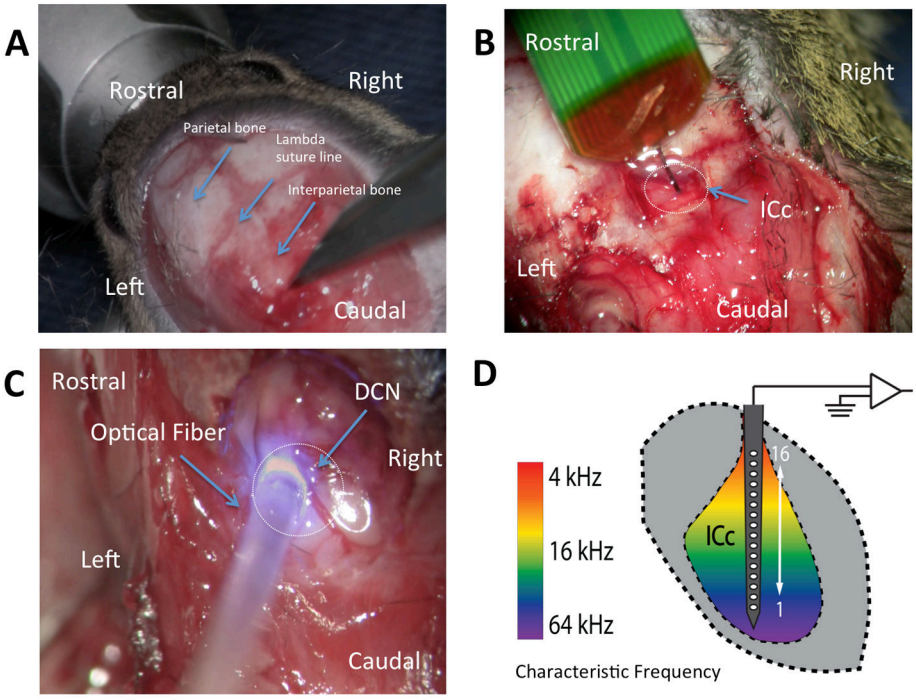

Figure 1. Surgical approach to the dorsal cochlear nucleus for opsin injection and for later positioning of optical fiber, and neural recording methods in the IC

A: The skin and muscle is retracted laterally to expose the lambda and coronal suture lines. **B**: Placement of NeuroNexus electrode probe into the IC in a vertical direction. **C:** Left-sided posterior craniotomy and partial cerebellar aspiration have been performed and a 400 μm diameter optical fiber mounted on a micromanipulator is introduced through the craniotomy and on the CN surface **D:** Schematic representation of the electrode probe positioned along the tonotopic axis of the central nucleus of the colliculus (ICc) so that each of the 16 electrodes records a different characteristic frequency.

Author Manuscript Author Manuscript Author Manuscript Author Manuscript

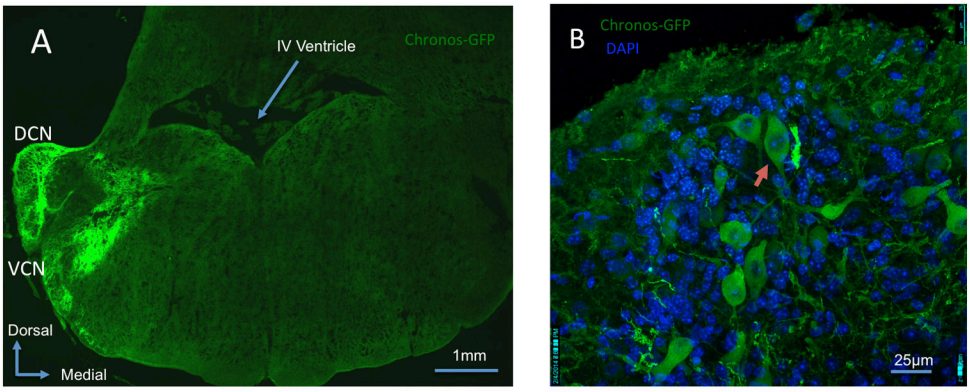

Figure 2. Chronos expression in the cochlear nucleus

A: Mosaic confocal 63x image showing Chronos-GFP expression within the dorsal cochlear nucleus (DCN) and ventral cochlear nucleus (VCN). **B:** Confocal 63x image of the DCN demonstrates Chronos-GFP expression within a fusiform cell (red arrow) and in other neuronal and non-neuronal populations. DAPI demonstrates all cell nuclei.

Author Manuscript Author Manuscript Author Manuscript Author Manuscript

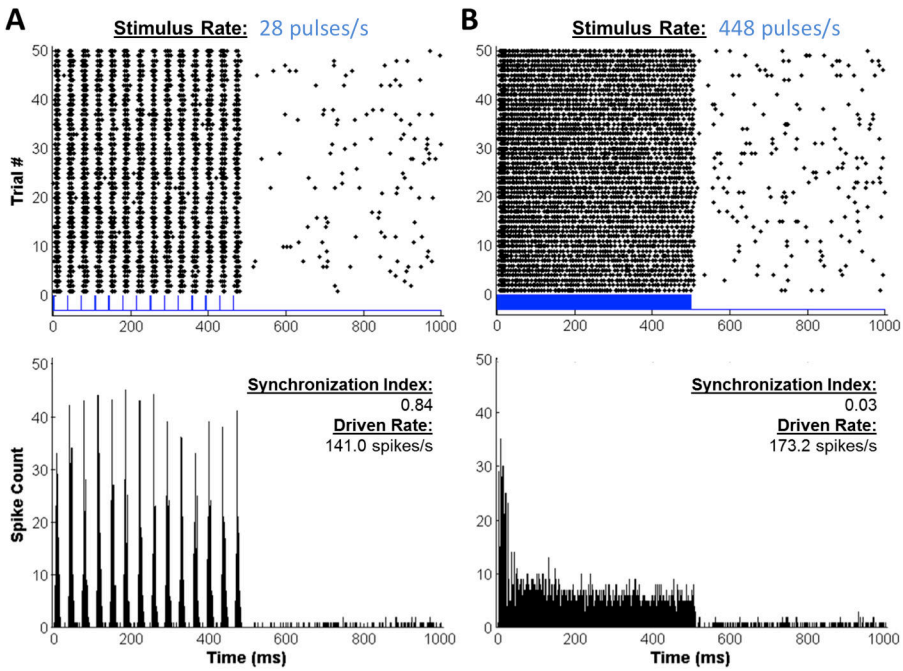

Figure 3. ICc neural activity evoked by light pulses

A: Responses at a low stimulus rate (28 pulses/s) elicit synchronized spikes (dots on raster plot at top). Bottom plot shows PST histogram for the same data. **B:** Responses at a high stimulus rate (448 pulses/s) show less synchrony (synchronization index given on the plots). In addition, the PST histogram shows the prominent rate adaptation during the pulse train. Driven rates (an average over the 500 ms duration pulse train) are indicated on the plots.

Author Manuscript Author Manuscript Author Manuscript Author Manuscript

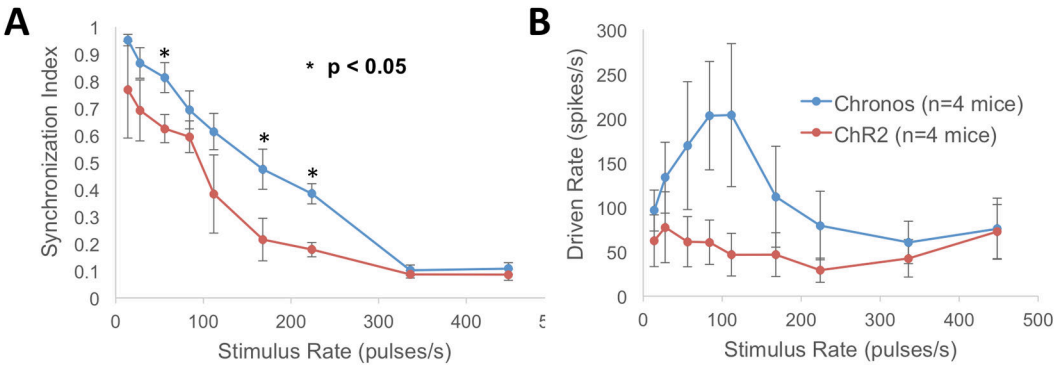

Figure 4. Synchronization index and driven rate as a function of pulse rate

A: Average SI over all 16 electrodes (at ~100 mW/mm^2) is significantly greater for Chronos than ChR2 at stimulus rates of 56, 168 and 224 pulses/s (* = $p < 0.05$, two-sample t-test). **B:** The maximum firing rates for Chronos and ChR2 (average +/− standard error).

Author Manuscript Author Manuscript Author Manuscript Author Manuscript

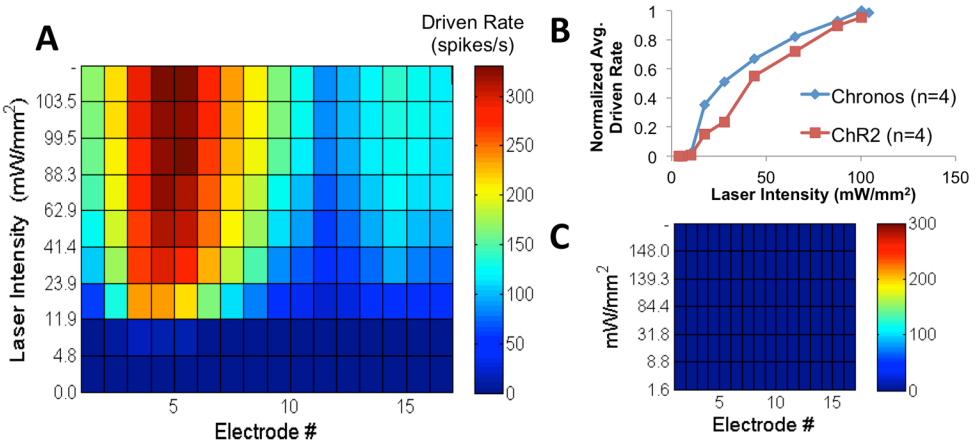

Figure 5. Broad pattern of laser-evoked neural activity as a function of recording position and stimulus intensity

A: Response map showing driven rate as a function of electrode (position in IC, see Fig. 1D) number and laser intensity. **B:** Plot of normalized driven rate across all electrodes as a function of laser intensity for the two opsins. **C:** Control mouse response map showing no driven response to light. Stimulus rate = 28 pulses/s.